Fast-Flow Study of the CH + CH Reaction Products

A. Bergeat, T. Calvo, G. Dorthe, and J.-C. Loison*

Laboratoire de Physico-Chimie Moléculaire, CNRS UMR No. 5803, Université Bordeaux I, F-33405 Talence Cedex, France

Received: November 5, 1998; In Final Form: May 14, 1999

The multichannel CH + CH reaction was studied, at room temperature, in a low-pressure fast-flow reactor. CH was obtained from the reaction of $CHBr_3$ with potassium atoms. An intense chemiluminescence from $C_2H(A^2\Pi)$ and a much weaker one from $C_2(d^3\Pi_g)$ were observed. The $C_2H(A^2\Pi)$ emission spectrum appeared as a continuum extending from 380 nm to the limit of our detection range at 800 nm. $C_2(d^3\Pi_g)$ was specifically produced in the $v = 2$ level, and the relative ratio $C_2(d^3\Pi_g)/C_2H(A^2\Pi)$ was proportional to the total pressure, this behavior being attributed to a production of C_2 by induced collision crossing states from excited vinylidene to the surface leading to $C_2(d^3\Pi_g) + H_2$. Relative product branching ratios were determined over the channels yielding the following atoms: H + C_2H, >90%; C + CH_2, <10%.

I. Introduction

CH radical is involved in combustion and interstellar chemistry.[1] However the CH + CH reaction was never experimentally studied in itself. Its rate was estimated to turn about $(1-4) \times 10^{-10}$ cm^3 molecule^{-1} s^{-1},[2] and it was proposed to be a contributor to the C_2H^* fluorescence continuum observed in the C_2H_2/O/H system.[3]

The product channel exothermicities[4] are given hereafter with respect to ground-state products:

$$CH + CH\ (+ M) \rightarrow C_2H_2\ (+ M) \qquad \Delta H^\circ_{298} = -10.00\ \text{eV} \quad (1)$$

$$(+ M) \rightarrow H_2CC\ (+ M) \qquad \Delta H^\circ_{298} = -7.98\ \text{eV} \quad (2)$$

$$\rightarrow C_2H + H \qquad \Delta H^\circ_{298} = -4.31\ \text{eV} \quad (3)$$

$$\rightarrow C_2 + H_2 \qquad \Delta H^\circ_{298} = -3.79\ \text{eV} \quad (4)$$

$$\rightarrow CH_2 + C \qquad \Delta H^\circ_{298} = -0.86\ \text{eV} \quad (5)$$

Ab initio calculations predict that the CH + CH reaction gives an energized C_2H_2 complex which dissociates into C_2H + H and to a lesser extent into $C_2 + H_2$ through the isomerization of (HCCH) into (H_2CC), C + CH_2 being a minor channel through the HCHC intermediate.[5]

A clean source of CH radicals (by the successive abstractions of Br atoms in $CHBr_3$ by K atoms) allowed study of this reaction in a fast-flow reactor. All the experiments were performed at room temperature. The chemiluminescent products (C_2H and C_2) were identified, and the branching ratios over the atomic channels (C_2H + H and CH_2 + C) were determined. These products were compared with the products of C_2H_2 excited by the Lymann-α radiation (121.56 nm)[6] to an energy similar to that of the intermediate C_2H_2 complex of the CH + CH reaction (Figure 1).

II. Experimental Section

A. Fast-Flow Reactor. The fast-flow reactor has been detailed elsewhere,[7] and only a brief description is thus given.

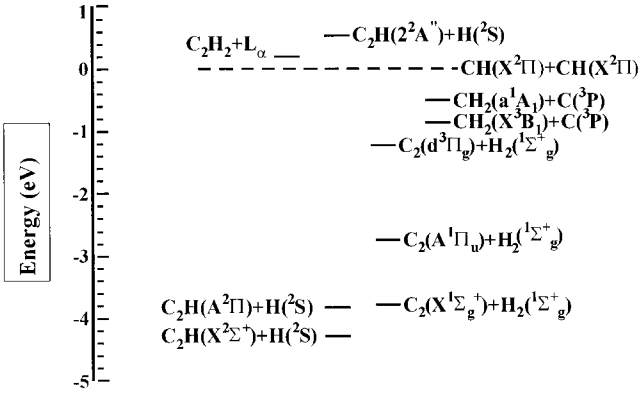

Figure 1. Energetic diagram of the CH + CH reaction and energy level of C_2H_2 excited by the Lyman-α radiation.

It consisted of a hollowed-out stainless steel block, with four perpendicular optical ports for detection by chemiluminescence and laser-induced fluorescence, in which a 36 mm inner diameter Teflon tube was inserted. The reactor was pumped by a Roots blower (Edwards EH 500) backed by a two-stage mechanical pump (Edwards E2M80). A 10.6 mm diameter diaphragm at the inlet of the Roots blower gave a flow velocity of 26.5 m s^{-1} for a total pressure of 2.0 Torr, the buffer gas being He with a purity > 99.995%. The reactant injector could slide along the Teflon inner wall of the reactor. The distance (d) between the window detection and the injector nozzle aperture could vary over the range 0−100 mm with a 0.5 mm precision. The pressure was measured by a capacitance manometer (Barocel 0−10 Torr), and the flow rates were adjusted by thermal mass flow meters (Tylan). As we did not know the precise concentration of CH radical in the reactor, the overall rate constant could not be determined. Since, in these experiments, CH was not mixed with other molecules or radicals, the inner diameter of the reactor could be reduced by a Teflon tube from 36 to 24.5 mm, the outer diameter of the potassium oven. In this configuration the reactant injector was used with or without the nozzle. In the latter case, the entire process of Br atom stripping from $CHBr_3$ to CH could be followed. So, we could distinguish the CH + CH and CH + CHBr contributions.

* Corresponding author. FAX: (33) 556846645. E-mail: jc@lpcm.u-bordeaux.fr.

10.1021/jp984311w CCC: $18.00
Published on Web 07/23/1999

Unfortunately, the wall reaction (due to the condensed potassium) was enhanced.

The detection of CH and CHBr radicals by laser-induced fluorescence has been previously described.[8]

The chemiluminescence signal from the reaction zone was collected by a quartz lens and dispersed over the 200−800 nm wavelength range by a Jobin-Yvon HRS2 monochromator using a 1200 g/mm grating blazed at 500 nm (3M210R) or 253.6 nm (2M210R). The wavelength responses with each of the gratings have been carefully recorded with a calibrated tungsten lamp (GAMMA Scientific Inc. RC-10A), and all spectra have been corrected. Atom detection by their resonance fluorescence in the vacuum UV has been previously detailed.[8] For H atoms, the relative density was determined from their fluorescence on the $^2P^0 \rightarrow {}^2S$ transition (Lyman-α) at 121.6 nm and for C atoms from their fluorescence on the $^3D^0 \rightarrow {}^3P$ transition at 156.1 nm and the $^3P^0 \rightarrow {}^3P$ transition at 165.7 nm.

B. Source of CH Radical. CH radicals were produced from the $CHBr_3 + 3K \rightarrow CH + 3KBr$ overall reaction which can be separated into the elementary steps:

$$CHBr_3 + K \rightarrow CHBr_2 + KBr \qquad \Delta_r H^\circ_{298} = -1.02 \pm 0.09 \text{ eV}\ ^9$$

$$CHBr_2 + K \rightarrow CHBr + KBr \qquad \Delta_r H^\circ_{298} = -0.77 \pm 0.1 \text{ eV}\ ^9$$

$$CHBr + K \rightarrow CH + KBr \qquad \Delta_r H^\circ_{298} = -0.38 \pm 0.2 \text{ eV}\ ^9$$

To characterize and optimize the CH production, the CH and CHBr radicals were probed by LIF when the different parameters, such as the oven temperature, the $CHBr_3$ flow, and the carrier-gas flow, were varied. The CHBr and CH experimental kinetics could be simulated by using for the successive Br atom abstractions the following rate constants: $(3 \pm 0.5) \times 10^{-10}$, $(0.9 \pm 0.5) \times 10^{-10}$, and $(3 \pm 2) \times 10^{-10}$ cm^3 molecule^{-1} s^{-1}, respectively. The simulation has already been given.[8]

The CH excitation spectrum showed that CH was produced only in the vibrational level $v = 0$ of the electronic ground state.[8]

III. Experimental Results

A. Chemiluminescent Products. *1. Chemiluminescences.* The CH + CH reaction gives a strong chemiluminescent continuum (380−800 nm) attributed to C_2H ($A^2\Pi \rightarrow X^2\Sigma^+$) and also some weaker emissions due to C_2 Swan bands ($d^3\Pi_g \rightarrow a^3\Pi_u$) and Phillips bands ($A^1\Pi_u \rightarrow X^1\Sigma^+_g$), as shown in Figure 2. K lines could also be observed. The C_2H emission spectrum has been first observed by Becker[10] from the photodissociation of C_2H_2 and then by Okabe,[11] Saito,[12] Suto,[6e] Shokooki,[13] and Sander,[14] from the photodissociation of C_2H_2 or C_2HBr. Shokooki et al.[13] have studied this fluorescence from visible to infrared wavelengths with filters and estimated that the major part was lying in the 1.0−2.75 μm region. This chemiluminescence was also observed in the system C_2H_2/O/H,[3] the CH + CH reaction supposedly being involved as well as the CH + CH_2 reaction.

2. Origin of the Chemiluminescences. Due to the relative complexity of the $CHBr_3$/K system, we checked that the observed chemiluminescences were not coming from reactions other than CH + CH. The kinetics of the successive K + $CHBr_x$ ($x = 3$ to 1) reactions have been simulated to fit the recorded variations with the time of the CH and CHBr concentrations.[8] $CHBr_3$ and $CHBr_2$ react quickly in the first millimeters with the usual K concentration, and their contributions could be neglected due to their low concentrations in the reactor. The only species which could remain at sufficiently high concentrations to react are CH radicals and possibly CHBr radicals. Then, the exoergic pathway leading to C_2 or C_2H could be

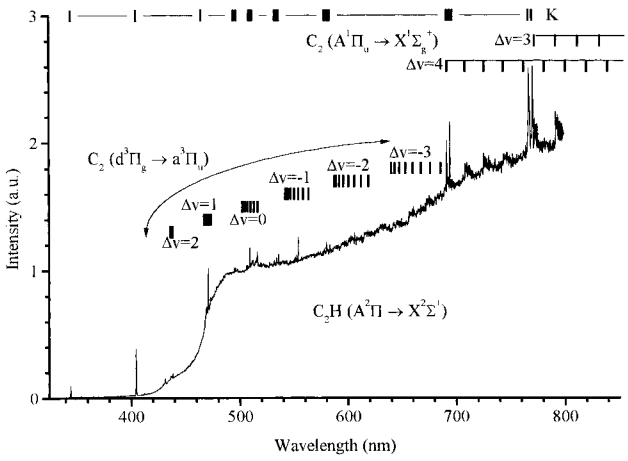

Figure 2. CH + CH chemiluminescences: $C_2H(A)$ continuum, $C_2(d)$ Swan bands, $C_2(A)$ Phillips bands, and K lines.

$$CH + CH \rightarrow C_2H + H \quad -4.31 \text{ eV} \quad (1a)$$

$$C_2 + H_2 \quad -3.79 \text{ eV} \quad (2a)$$

$$CH + CHBr \rightarrow C_2H + HBr \quad -4.54 \text{ eV} \quad (1b)$$

$$C_2H + H + Br \quad -0.82 \text{ eV} \quad (2b)$$

$$C_2 + H_2 + Br \quad -0.32 \text{ eV} \quad (3b)$$

The first channel of either reaction is sufficiently exoergic to produce excited C_2H, but only the second channel of CH + CH reaction is sufficiently exoergic to produce excited C_2 in either of $A^1\Pi_u$ and $d^3\Pi_g$ states. The CHBr + CHBr reaction could not give excited C_2H or C_2. With application of the steady-state approximation to excited C_2H or C_2 radicals, the following expressions are obtained for the radiative species concentrations:

$$[C_2H^*] = \frac{k^{1*}_{CH+CH}[CH]^2 + k^{1*}_{CH+CHBr}[CH][CHBr]}{k_e + k_Q[He]}$$

$$[C_2^*] = \frac{k^{2*}_{CH+CH}[CH]^2}{k_e + k_Q[He]}$$

Under our helium pressure, the quenching pseudo-first-order rate constant k_Q[He] was actually negligible with respect to the emission rate constant k_e for $C_2(d^3\Pi_g)$.[12,14] By subtracting the C_2H continuum, we obtained the $C_2(d^3\Pi_g)$ chemiluminescence spectrum (Figure 3). An unusual intensity of the emission from $v = 2$ could be observed. The intensity of that level was always proportional to $[CH]^2$, which was not the case for the weaker signal from $v = 0$ which could be partially populated by the C + CH reaction. This point will be discussed later. In Figure 4a, the C_2H and $C_2(d^3\Pi_g, v=2)$ chemiluminescence signals and the CH and CHBr LIF signals are plotted against the $CHBr_3$ concentration for a potassium concentration evaluated to 2 mTorr. At the beginning of the curve, the $CHBr_3$ concentration was much less than the K concentration and the three strippings of Br atoms in $CHBr_3$ were fast, in order that only CH radicals were present in the reactor. When the $CHBr_3$ concentration was greater than 0.1[K], the kinetics of the last abstraction (CHBr

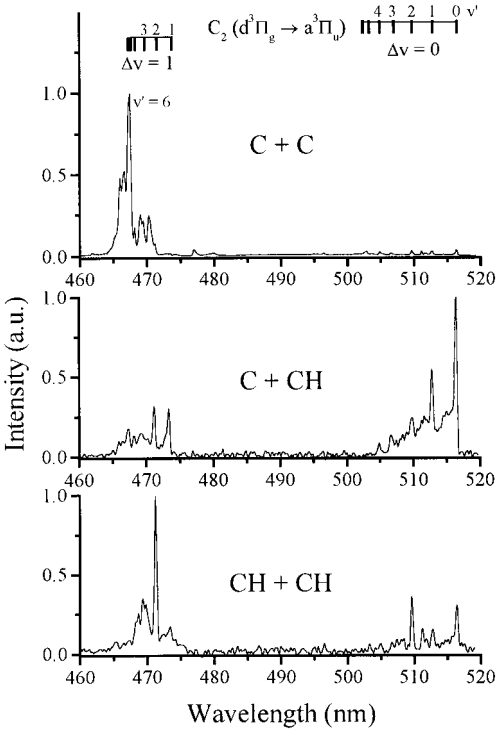

Figure 3. Normalized $C_2(d3\Pi_g)$ chemiluminescence spectra given by the C + C, C + CH, or CH + CH reactions (the C_2H continuum has been subtracted).

+ K → CH + KBr) was too slow for full conversion of $CHBr_3$ into CH and the CH concentration was no more proportional to the introduced $CHBr_3$ concentration. The $C_2(d^3\Pi_g,v=2)$ and C_2H signals actually were proportional to $[CH]^2$ whatever the $CHBr_3$ concentration and thus the CHBr concentration. The contribution of any reaction involving CHBr appears negligible, not only for the C_2 chemiluminescence as expected but also for the C_2H chemiluminescence.

This is also seen in Figure 4b which gives both the evolution of the CH radical concentration and those of the C_2H and C_2 chemiluminescence signals against the distance in the reactor used without the nozzle and with $[K] \approx 10 \times [CHBr_3]$. In this case, all the reactions of potassium with $CHBr_3$ occurred in the reactor. At a distance of 1.2 cm, $CHBr_3$ had been completely converted into CH and KBr. After, the CH decrease was due to the CH + CH reaction and the wall reactions. The $C_2(d^3\Pi_g,v=2)$ and C_2H chemiluminescence signals here again were proportional to $[CH]^2$. There is no doubt that the C_2H^* and the $C_2(d^3\Pi_g,v=2)$ chemiluminescence were given by the CH + CH reaction. The fact that the CH + CHBr reaction does not give C_2H^* + HBr, despite the exoergicity of the channel leading to C_2H + HBr, suggests that the reaction CH + CHBr produces mainly C_2H_2 + Br (and possibly C_2HBr + H) and not C_2H + HBr.

3. Internal Distribution of Energy. $C_2H(A^2\Pi)$. The detection of the chemiluminescence was limited by our experimental setup to the range 200−800 nm (Figure 2), although the $C_2H(A^2\Pi)$ emission spectrum extends into the infrared.[13] Moreover, the emitting vibrational levels and thus their oscillator strengths were unknown. Then, the relative branching ratio between $C_2H(A^2\Pi)$ and $C_2(d^3\Pi_g)$ could not be determined but could only be roughly estimated as $C_2H(A^2\Pi)/C_2(d^3\Pi_g) > 100$ at 1.5 Torr. The recorded part of the C_2H^* spectrum, with CH concentration estimated to 0.01 mTorr, has been compared with the OH* spectrum coming from the CH + O_2 reaction with O_2 pressure of 1.00 mTorr. The C_2H^* branching ratio exceeds that of the

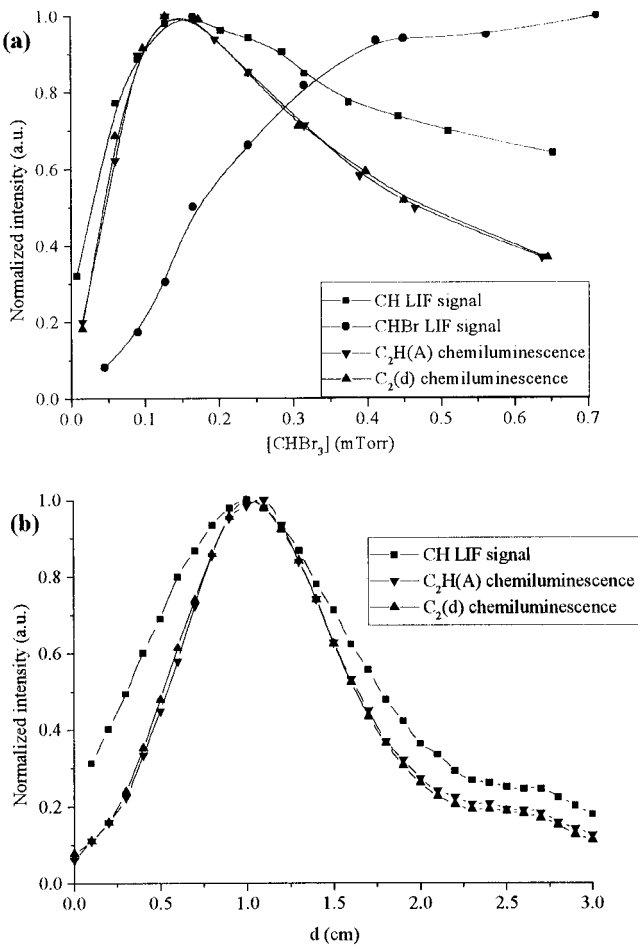

Figure 4. (a) Normalized intensity evolutions of the CH and CHBr laser-induced fluorescence and the $C_2H(A)$ and $C_2(d)$ chemiluminescences versus the $CHBr_3$ concentration introduced in the reactant injector (observation distance $d = 0.5$ cm, reaction delay in the nozzle dc = 0.8 cm and $[K] \approx 2$ mTorr. (b) Normalized intensity evolutions of the CH laser-induced fluorescence and the $C_2H(A)$ and $C_2(d)$ chemiluminescences versus the observation distance d (flow velocity ≈ 2600 cm s^{-1}), the injector being without nozzle (dc = 0 cm).

OH* one by a factor of 10−100. Since the CH + O_2 → OH* + CO branching ratio has been estimated to 0.48%,[3] we could estimate that the C_2H^* branching ratio is equal to at least a few percent (from the recorded visible part of the chemiluminescence) and must actually be much greater, depending on the ratio of the recorded visible emission to the total emission of C_2H. Such a branching ratio for a chemiluminescent pathway is unusual.

Even with a resolution of 0.09 nm, the emission of C_2H^* appeared structureless. That should be due to the high-level density of the A state combined with an overlapping of the different rovibronic A−X transitions. A steep decrease of the intensity occurred around 490 nm (2.53 eV). At 380 nm, the signal became buried in the noise, but that wavelength was not a sharp limit since the signal seemed to still continue to fade out very slowly with decreasing wavelength, becoming totally indistinguishable at about 340 nm. According to the channel exoergicity, 4.31 eV, the chemiluminescence limit should be at 288 nm. The disappearance of the signal, much below the expected limit, could proceed from a lack of radical population above 3.3 eV or to a strong decrease of the rovibronic transition probabilities from levels above 3.3 eV. The chemiluminescence spectrum of C_2H^* shows no change with the pressure in the range 0.500−5.000 Torr, while the lifetime of $C_2H(A)$ is

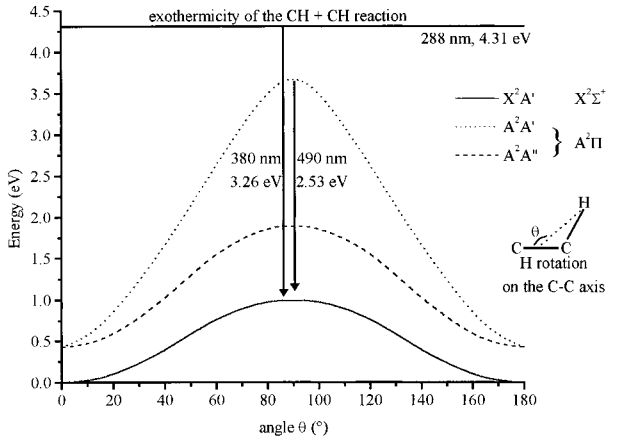

Figure 5. Ab initio calculations on the isomerization barriers in $C_2H(X^2\Sigma^+)$ and $C_2H(A^2\Pi)$ by Boggio-Pasqua and Halvick,[16] which could explain the experimental decrease of the chemiluminescence signal at 490 nm and its cutoff at 380 nm.

between 5 and 60 μs.[12,13] This indicates that the relaxation does not change the population distribution spectrum and, in particular, that the emission limit is not due to a removal of the population of higher levels by collisional relaxation.

The atomic hydrogen velocity distribution obtained in the photodissociation of C_2H_2 at Lyman-α wavelength by Lai et al.[6b] and Zhang et al.[15] showed an important contribution of small velocities associated with a production of C_2H mainly in the excited A state. The comparison between the CH + CH reaction and the photodissociation of C_2H_2 at the Lyman-α wavelength (121 nm) is difficult due to the lack of theoretical information about the CH + CH reaction particularly on the multiplicity of C_2H_2 (either in singlet or triplet state) produced in the addition step (the excitation of C_2H_2 at Lyman-α promotes C_2H_2 in the $3R''(^1\Pi_u)2^1_0$ and the $^2CH + {}^2CH$ reaction could produce $^1C_2H_2$ or $^3C_2H_2$). Nevertheless, since $C_2H(A)$ is produced in both cases with a similar available energy and since the emission spectra are very similar, it is reasonable to think that $C_2H(A)$ is populated up to the population limit set by the exoergicity of the CH + CH → C_2H + H channel. The extremely weak signal, well below the expected limit, should thus be due to a sharp decrease of the transition probabilities. This conclusion is consistent with Boggio-Pasqua and Halvick's ab initio calculation of the C_2H potential energy surface.[16] An isomerization barrier of 1 eV, for the X state, and 3.6 eV, for the A state (Figure 5), have been found. Above these limits, the vibronic wave functions are delocalized with a small maximum just above the barrier. Then, the Franck−Condon factors become small for transitions between $E(A) > 3.6$ eV and $E(X) > 1$ eV (which corresponds to the decrease of the signal at 480 nm) and very small for transitions between $E(A) > 3.6$ eV and $E(X) < 1$ eV.

$C_2(d^3\Pi_g)$ Vibrational Distribution. The exoergicity of the CH + CH → C_2 + H_2 channel allows one to populate $C_2(d^3\Pi_g)$ up to $v = 6$. The $C_2(d^3\Pi_g)$ chemiluminescence spectrum showed an unusually intense signal from $v = 2$, the second in importance being that from $v = 0$ (Figures 4 and 6). It was kinetically demonstrated that $C_2(d^3\Pi_g)$, $v = 2$, was actually produced by the CH + CH reaction while we could not check it for $v = 0$ which could thus be partially filled by other exoergic reactions such as C + CH → C_2 + H and C + C + M → C_2 + M, C atoms being produced by CH + CH → CH_2 + C or by CH + CH → C_2H + H followed by H + CH → C + H_2. The termolecular reaction C + C + (M) is known to produce $C_2(d^3\Pi_g)$ high-pressure bands characterized by a prominent

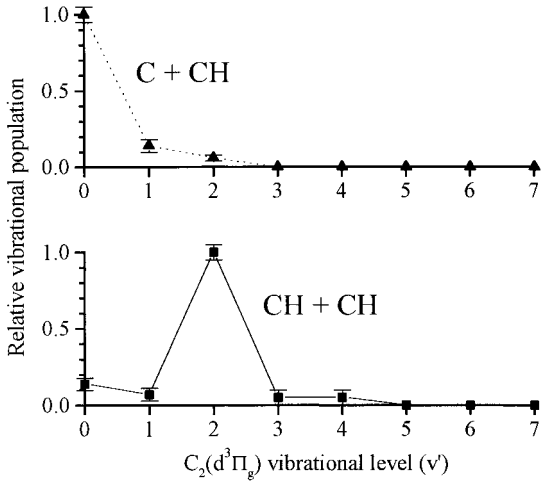

Figure 6. Relative $C_2(d3\Pi_g)$ vibrational population distribution given by the C + CH and CH + CH reactions.

emission from $v = 6$.[17] It results that this reaction cannot contribute to $v = 0$ and even to $v = 2$, except a significant collisional relaxation decreasing $v = 6$ to the benefit of lower levels. To check it, C atoms were produced by the successive abstraction of Cl atoms in CCl_4 by potassium[18] (since the C + CCl → C_2 + Cl reaction is not sufficiently exoergic to produce $C_2(d^3\Pi_g)$, the only reaction able to produce $C_2(d^3\Pi_g)$ is the C + C + M reaction). We actually recorded C_2 high-pressure bands with emission from $v = 6$ as expected, those from $v = 0$ and $v = 2$ being negligible (Figure 3). The C + C + M reaction could thus be discarded. Then, we observed the modification of the chemiluminescent spectrum by introducing a contribution of the C + CH reaction. For that purpose, a mixture of CCl_4 and $CHBr_3$ precursors was used. The spectrum changes according to the proportions of CCl_4 and $CHBr_3$. For weak relative concentrations of CCl_4, we tended to recover the chemiluminescence spectrum of CH + CH, and for strong relative concentrations of CCl_4, we tended to recover the chemiluminescence spectrum of C + C + M. We could obtain a spectrum (Figure 3) ascribed mainly to C + CH with minor contributions of CH + CH and C + C + M. The corresponding vibrational distribution is given in Figure 6. The population decreases from $v = 0$ to $v = 2$ in agreement with the exoergicity of the reaction C + CH, which allows population up to $v = 2$. However, the weak population of $v = 2$ could partly be due to CH + CH which could not be completely removed, the latter reaction producing more specifically that level. The actual population of $v = 2$ by C + CH should be negligible with respect to that of $v = 0.1$. The comparison with all these experiments suggests that in the experiments with $CHBr_3$ alone, used for the CH + CH reaction, the contribution from C + C + M and C + CH to $v = 2$ should be negligible, which explains that the signal from that level was found to be proportional to $[CH]^2$. In return, $v = 0$, whose signal intensity was not proportional to $[CH]^2$, was partially populated by C + CH. From the evolution with the time of C atom and CH radical densities, we determined the nascent vibrational distribution of $C_2(d^3\Pi_g)$ produced by the CH + CH reaction (Figure 6). This distribution shows a very specific production of $v = 2$. A second feature to point out was the linear increase of the $C_2^*(v'=2)/C_2H(A)$ ratio with the total pressure (Figure 7).

Such a vibrational population distribution in $C_2(d^3\Pi_g)$, peaking at $v = 2$ and being pressure dependent, is characteristic of a collisional transfer from a nonradiative level to $C_2(d^3\Pi_g, v'=2)$, as it occurs for the case of high-pressure bands peaking at $v = 6$ due to the transfer from $C_2(^5\Pi_g, v=0)$ to C_2-

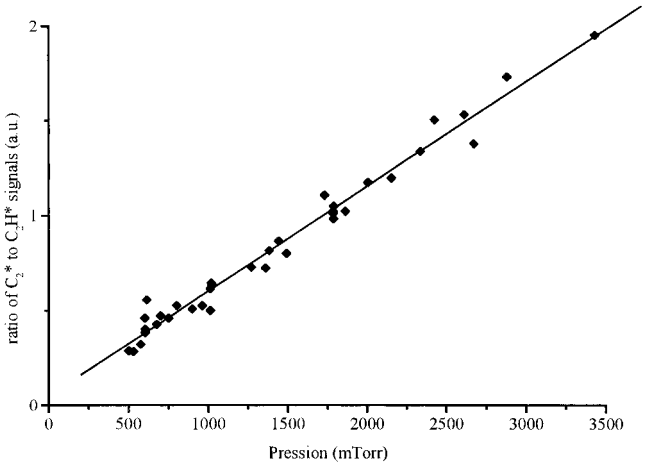

Figure 7. Ratio of the $C_2(d3\Pi_g,v'=2\rightarrow a3\Pi_u,v=1)$ chemiluminescence signal to the C_2H ($A^2\Pi \rightarrow X^2\Sigma^+$, around 480 nm) chemiluminescence signal versus the total pressure in the reactor.

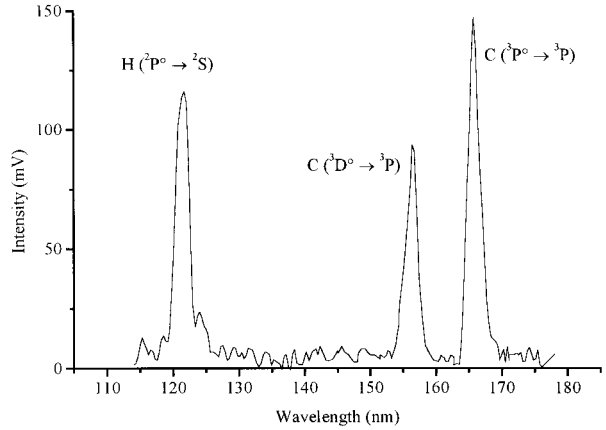

Figure 8. Typical maximal atomic resonance fluorescence spectrum during the CH + CH reaction study (lamp line intensities were as follows: H, 1.00; C (156 nm), 7.00; and C (165 nm), 4.30).

$(d^3\Pi_g,v=6)$.[19] As there is no corresponding crossing state in C_2 allowing a specific transfer to $d^3\Pi_g(v'=2)$, this transfer should proceed from another way. We propose a transfer which could stem from the crossing of an excited state of CCH_2 (vinylidene) with the $C_2(d^3\Pi_g) + H_2$ surface specifically at the level of $v = 2$, CCH_2 coming from an isomerization of C_2H_2 produced by the CH + CH reaction. The increase of the C_2*/C_2H* ratio with pressure indicates that this transfer is collision induced. For comparison, it may be noticed that in the case of the vacuum UV photodissociation of C_2H_2, the channel leading to H + C_2H has been estimated to 10−30%,[6c] while CCH_2 has been detected in absorption.[6d] As will be shown later, the main pathway leading to atoms is the H + C_2H pathway.

B. Atomic Branching Ratio. To determine the product branching ratios over the channels yielding H + C_2H and C + CH_2, the H and C atoms were probed by their resonance fluorescence in the vacuum UV. First, it was checked that the atomic absorption was small. In this condition, the fluorescence signal divided by the emission intensity was proportional to (f_A/δ_A)[A], [A] being the atomic concentration, f_A the oscillator strength,[20] and δ_A the Doppler broadening ($T = 300$ K).[21] A typical atomic fluorescence spectrum, at a distance of 1.5 cm, is shown in Figure 8. Examples of the evolutions of the CH radical and C and H atom fluorescence intensities are given normalized to their maximum in Figure 9. The fact that the C atom density rise is delayed with respect to that of H atoms shows clearly that the probed C density, proceeding at the

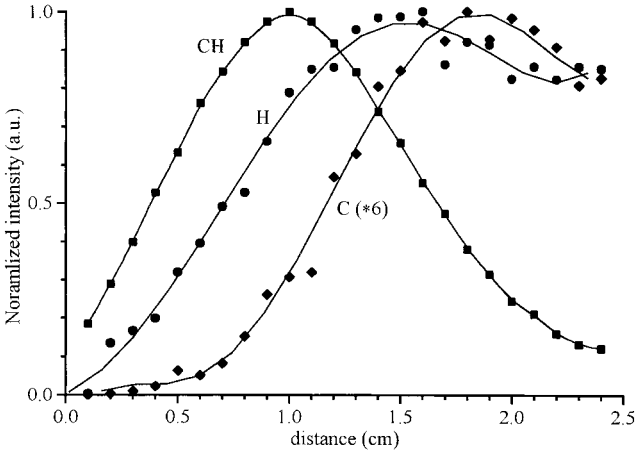

Figure 9. Kinetics of the CH laser-induced fluorescence signal and H and C atomic resonance fluorescence (ARF) signals. All signals are normalized to their maximum. The C density maximum is actually 6 times lower than that of H.

beginning from the CH + CH → CH_2 + C reaction, benefits later from the increasing contribution of the H + CH → C + H_2 reaction, H being produced by the main reaction channel CH + CH → C_2H + H. The ratio between the maximum densities of hydrogen atoms and carbon atoms which is actually equal to 6 is thus lower than the ratio of the production rates of these atoms by the CH + CH reaction. Actually, the ratio of the slopes at the origin of the atom density evolutions which should reflect the ratio of their production rates is about 30 corresponding thus to 97% C_2H + H and 3% CH_2 + C which should thus be a very minor channel. Due to the uncertainties attached to our experiments, we cannot put forward a precise branching value but we can ascertain that the branching ratio between C_2H + H and CH_2 + C is ≥90% in favor of C_2H + H, in full agreement with the suggestion, from a theoretical analysis of the CH + CH reaction,[5] that the channel leading to CH_2 + C should be of no importance.

IV. Conclusion

Our efficient CH radical source allowed us to study the CH + CH reaction. We determined that the branching ratio between C_2H + H and CH_2 + C was ≥90% in favor of C_2H + H, in agreement with theoretical investigations[5] concluding that C_2H + H should be the main product channel of the CH + CH reaction, followed by C_2 + H_2, C + CH_2 being a minor channel. We also observed a strong chemiluminescence of C_2H without any pressure dependence of the emission spectrum. The C_2H emission spectrum appeared identical to that previously observed from the vacuum UV Lyman-α photodissociation of C_2H_2, excited at an energy level very close to that of C_2H_2 formed as a complex of the CH + CH reaction. We observed a pressure dependent chemiluminescence of C_2 ($d^3\Pi_g$) specifically produced by CH + CH in the vibrational level $v = 2$. Such specificity was not previously observed in other cases of C_2 ($d^3\Pi_g$) chemiluminescence and cannot be explained by a collision-induced transfer between C_2 vibronic states. We imagine that it reflects some collision-induced transfer in the energetized vinylidene complex leading to its dissociation into C_2 ($d^3\Pi_g,v=2$) + H_2.

References and Notes

(1) (a) Lindqvist, M.; Sandqvist, A.; Winnberg, A.; Johansson, L.; Nyman, L-Å. *Astron. Astrophys. Suppl. Ser.* **1995**, *113*, 257. (b) Rieu, N.-Q.; Henkel, C.; Jackson, J.; Mauersberger, R. *Astron. Astrophys.* **1991**, *241*, 233.

(2) Dean, A. J.; Hanson, R. K. *Int. J. Chem. Kinet*. **1992**, *24*, 517.
(3) Grebe, J.; Homann, K. *Ber. Bunsen-Ges. Phys. Chem.* **1982**, *86*, 587.
(4) The channel exothermicities are calculated using handbook values or Janaf table values for $\Delta_f H°_{298}$ except for C_2H_2 (Mordaunt, D. H.; Ashfold, M. N. *J. Chem. Phys.* **1994**, *101*, 2630) and CCH_2(vinylidene) (Ervin, K. M.; Ho, J. H.; Lineberger, W. C. *J. Chem. Phys.* **1989**, *91*, 5974).
(5) Shen, D.; Pritchard, H. O. *Theor. Chim. Acta* **1991**, *78*, 241.
(6) (a) Löfler, P.; Lacombe, D.; Ross, A.; Wrede, E.; Schneider, L.; Welge, K. H. *Chem. Phys. Lett.* **1996**, *252*, 304. (b) Lai, L.-H.; Che, D.-C.; Liu, K *J. Phys. Chem.* **1996**, *100*, 6376. (c) Seki, K.; Okabe, H. *J. Phys. Chem.* **1993**, *97*, 5284. (d) Laufer, A. H. *Chem. Phys. Lett.* **1983**, *94*, 240. (e) Suto, M.; Lee, L. C. *J. Chem. Phys*. **1984**, *80*, 4824.
(7) Daugey, N.; Bergeat, A.; Schuck, A.; Caubet, P.; Dorthe, G. *Chem. Phys.* **1997**, *222*, 87.
(8) Bergeat, A.; Calvo, T.; Loison, J.-C.; Dorthe, G. *J. Phys. Chem.*, in press.
(9) (a) Born, M.; Ingemann, S.; Nibbering, N. *J. Am. Chem. Soc.* **1994**, *116*, 7210. (b) Tschuikow-Roux, E.; Paddison, S. *Int. J. Chem. Kinet.* **1987**, *19*, 15.
(10) Becker, K. H.; Haaks, D.; Schurgers, M. *Z. Naturforsch. A* **1971**, *26*, 1770.
(11) Okabe, H. *J. Chem. Phys.* **1975**, *62*, 2782.
(12) Saito, Y.; Hikida, T.; Ichimura, T.; Mori, Y. *J. Chem. Phys*. **1984**, *80*, 31.
(13) Shokoodi, F.; Watson, T. A.; Reisler, H.; Kong, F.; Renlund, A. M.; Wittig, C. *J. Phys. Chem.* **1986**, *90*, 5695.
(14) Sander, R. K.; Tiee, J. J.; Quick, C. R.; Romero, R. J.; Estler, R. *J. Chem. Phys.* **1988**, *89*, 3495.
(15) Zhang, J.; Riehn, C. W.; Dulligan, M.; Wittig, C. *J. Chem. Phys.* **1995**, *103*, 6815.
(16) Boggio-Pasqua, M.; Halvick, P. Private communication.
(17) Caubet P.; Dorthe G. *Chem. Phys. Lett.* **1994**, *218*, 529.
(18) Bergeat, A.; Calvo, T.; Loison, J.-C.; Dorthe, G. Manuscript in preparation.
(19) Little, C. E.; Browne, P. G. *Chem. Phys. Lett* **1987**, *134*, 560.
(20) Wiese, W.; Fuhr, J.; Deters, T. *J. Phys. Chem. Ref. Data* **1996**, *7*.
(21) Lynch, K.; Schwab, T.; Michael, J. *Int. J. Chem. Kinet*. **1976**, *8*, 651.